# Novel Poly(Ethylene Oxide)-*b*-Poly(Propylene Oxide) Copolymer-Glucose Conjugate by the Microwave-Assisted Ring Opening of a Sugar Lactone[a]

Romina J. Glisoni, Alejandro Sosnik*

In this work, we investigated for the first time the conjugation of gluconolactone to a poly(ethylene oxide)-poly(propylene oxide) block copolymer by a microwave-assisted ring opening reaction. The glucosylated copolymer was obtained with high yield (90%). A conjugation extent of approximately 100% was achieved within 15 min. The modification reduced the critical micellar concentration and increased the size of the micelles. The agglutination of the modified polymeric micelles by a soluble lectin that binds glucose confirmed the recognizability of the modified nanocarrier. Finally, the solubilization of darunavir, an anti-HIV protease inhibitor, showed a sharp increase of the aqueous solubility from 91 microgram/mL to 14.2 and 18.9 mg/mL for 10% w/v pristine and glucosylated polymeric micelles, respectively.

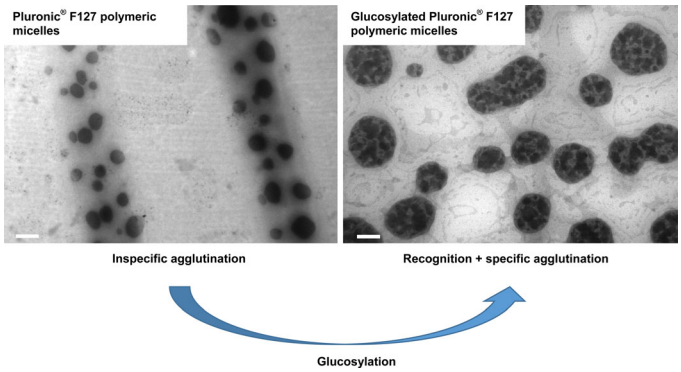


## 1. Introduction

Macrophages are pivotal players in the host innate and adaptive immune responses and they are involved in different inflammatory diseases (e.g., inflammatory bowel disease).[1,2] In addition, the macrophage is the cellular host of a variety of intracellular pathogens such as the non-replicating form of *Mycobacterium tuberculosis*.[3] In the same way, the human immunodeficiency virus (HIV)[4] and protozoa (e.g., leishmania)[5] colonize this cell population and, by doing so, perpetuate the infection. The modification of nanocarriers with ligands that are selectively recognized by receptors in the target cell reduces the systemic exposure to the drug and the associated adverse effects and increases the therapeutic index. In this scenario, there exists special interest in conceiving novel and translatable drug delivery platforms that would enable (i) the selective targeting of active agents to control the proliferation and the activation

Dr. R. J. Glisoni
The Group of Biomaterials and Nanotechnology for Improved Medicines (BIONIMED), Department of Pharmaceutical Technology, Faculty of Pharmacy and Biochemistry, University of Buenos Aires, Buenos Aires CP1113, Argentina
National Science Research Council (CONICET), Buenos Aires, Argentina
Prof. A. Sosnik
Group of Pharmaceutical Nanomaterials Science, Department of Materials Science and Engineering, Technion-Israel Institute of Technology, Technion City 32000, Haifa, Israel
Department of Materials Science and Engineering, De-Jur Building, Office 607, Technion-Israel Institute of Technology, Technion City 32000, Haifa, Israel
E-mail: alesosnik@gmail.com

[a]**Supporting Information** is available from the Wiley Online Library or from the author.

of macrophages in different body sites and (ii) to attack intracellular pathogens.

Lectin-like receptors (LLRs) are transmembrane proteins with single or multiple carbohydrate high-affinity binding sites and selectivity.[6–9] The mannose receptor is a type-I transmembrane C-type lectin[10,11] that binds mannose, fucose, and glucose with variable affinity.[12] Macrophages present a high concentration of LLRs on the outer membrane surface that enables the recognition of sugar motifs in pathogens and their subsequent phagocytosis.[6,13] In this context, nanocarriers surface-modified with mannose have emerged as an appealing tool to target drugs to macrophages by diverse administration routes.[14–19]

Polymeric micelles (PMs) are a unique kind of self-assembled nanostructure formed by the spontaneous aggregation of amphiphilic block copolymers above the critical micellar concentration (CMC).[20,21] They are formed by two main domains, an inner lipophilic core and an outer hydrophilic corona. The core enables the solubilization and/or physicochemical stabilization of hydrophobic drugs in aqueous medium, while the corona stabilizes the system and serves as a barrier between the external medium and the core. Unmodified PMs have been also investigated to target tumors by the enhanced permeation and retention effect.[22] Due to the great chemical versatility and the ability to fine tune their features, PMs have emerged as one of the most promising nano-drug delivery systems (nano-DDS)[23–25] and, over the last decades, they have led to a profuse intellectual property.[26]

Poly(ethylene oxide)–poly(propylene oxide) (PEO–PPOs) block copolymers are thermo-responsive amphiphiles that have been extensively investigated as drug nanocarriers.[27,28] Owing to the good cell and biocompatibility, some derivatives have been approved by the US Food and Drug Administration (US FDA) for use in pharmaceutical products and medical devices. PEO–PPOs are commercially available in two different molecular architectures, the linear poloxamers (Pluronic®) and branched poloxamines (Tetronic®), and a broad spectrum of molecular weights and hydrophilic–lipophilic balances.[27] Our group has extensively investigated the use of pristine and modified PEO–PPOs for the encapsulation, release, and targeting of drugs by the topical, the oral, the parenteral, and the intranasal route[29–38] and also the PEO–PPO-mediated inhibition of the activity of pumps of the ATP-binding cassette superfamily.[39–42] Irrespective of their potential, the ability of pristine PMs to target specific cell types is remarkably constrained due to the PEGylated nature of the surface that minimizes interaction with phagocytic cells. The coating of polymeric nanocarriers with sugar residues not only would stabilize the colloidal system due to formation of multiple hydrogen bonds in the micellar corona, but would also favor its receptor-mediated internalization by the target cell.[43] To improve the binding of PEO–PPO micelles to LLRs expressed by hepatocytes, their surface was modified with lactobionic acid (an oxidized derivative of lactose) employing the conventional Steglich esterification reaction.[44] Lactosylated micelles were used to encapsulate nitazoxanide,[45] an antimicrobial and immunomodulator drug clinically trialed for the treatment of chronic hepatitis B.[46] However, this chemical pathway led to conjugation extents that were quite low and that depended on the block copolymer architecture and its molecular weight.[44,47] Furthermore, the long reaction time (72 h) and the inability to control and/or fine tune the modification extent represent serious drawbacks toward the scale-up and the bench-to-bedside translation. In this framework, we are interested in exploring faster, more tunable and scalable synthetic pathways for the production of PEO–PPO-sugar conjugates.

Microwave radiation has emerged as a valuable tool for the synthesis of polymeric biomaterials.[48] One of the most extensively explored reactions has been the ring opening polymerization of epsilon-caprolactone that led to significantly faster reactions than the conventional methods.[49,50] In the present work, we investigated for the first time the microwave-assisted ring opening reaction of gluconolactone employing the terminal –OH groups of Pluronic® F127 as initiator. A derivative with approximately 100% substitution extent (2 glucose molecules per copolymer) was produced within 15 min and with very high yield (90%). In addition, the resulting PMs showed improved self-aggregation tendency and underwent fast agglutination in the presence of a soluble lectin, positioning this new derivative as a promising platform for further drug encapsulation and active targeting investigations. Finally, the solubilization of darunavir free base (DRV), a protease inhibitor used to treat the HIV infection, was assessed for the first time in a polymeric nanocarrier with very promising results.

## 2. Experimental Section

### 2.1. Materials

Pluronic® F127 (F127, $\overline{M}_w = 12\,600\ g \cdot mol^{-1}$; PEO weight content, % PEO = 70%; hydrophilic–lipophilic balance of 18–23), was a gift of BASF Corporation (New Milford, CT, USA) and it was dried under vacuum (100–120 °C in oil bath, 2 h) before use. In the synthetic stage, the copolymer was used without further purification, while in all the physicochemical and aggregation characterizations, it was previously dialyzed against distilled water (regenerated cellulose dialysis membranes; molecular weight cut-off of $3\ 500\ g \cdot mol^{-1}$, Spectra/Por® 3 nominal flat width of 45 mm, diameter of 29 mm, and volume/length ratio of $6.4\ mL \cdot cm^{-1}$; Spectrum Laboratories,



Macromol. Biosci. 2014, DOI: 10.1002/mabi.201400235

Inc., Rancho Dominguez, CA, USA) over 48 h and freeze-dried (see below). Gluconolactone (Glu; 1,2,3,4,5-pentahydroxycaproic acid δ-lactone, molar mass = 178.14 g · mol$^{-1}$) and tin(II) 2-ethylhexanoate (catalyst, Sn(Oct)$_2$, 95%) were purchased from Sigma–Aldrich (St. Louis, MO, USA) and used as received. Dimethylformamide (DMF, Sigma–Aldrich) was used as the reaction solvent and dried with activated molecular sieves 3A (Sigma–Aldrich) for at least 48 h. Darunavir free base (DRV, Figure S1A) was isolated from commercially available Prezista® tablets (Janssen-Cilag, Titusville, NJ, USA) containing 650.46 mg of darunavir ethanolate (equivalent to 600 mg of darunavir free base) using dichloromethane (DCM) as the extraction solvent. The purity of the isolated DRV was confirmed by $^1$H- and $^{13}$C NMR spectroscopy (Figure S1B), employing deuterated dimethylsulfoxide (DMSO-$d_6$) in a 500-MHz Bruker® Avance II High Resolution spectrometer) and Bruker TOPSPIN 2.1 software (Bruker BioSpin GmbH, Rheinstetten, Germany), melting point analysis (Fisher-Johns Melting Point Apparatus, Thermo Fisher Scientific, Inc., Waltham, MA, USA) and compared to a DRV standard kindly provided by Laboratorios Richmond (Buenos Aires, Argentina). All the other solvents were of analytical or spectroscopic quality and used without further purification.

### 2.2. Microwave-Assisted Glucosylation of PEO–PPO

The conjugation of Glu to the terminal —OH of F127 was performed by the microwave-assisted ring opening reaction of gluconolactone in presence of Sn(Oct)$_2$ using a household microwave oven (Itedo™, radiation frequency 2.45 GHz, potency 900 W, Shanghai, China) with five power levels (10, 30, 50, 80, and 100). The oven was adapted to setup a condenser. In brief, dry F127 (5.0 g, see above) and gluconolactone (155 mg, 10% molar excess) were dissolved in anhydrous DMF (10 mL) under magnetic stirring. Sn(Oct)$_2$ (130 μL, 1:1 molar ratio to F127) was added and the round-bottom flask was placed in the center of the microwave oven and connected to the condenser.[49,50] The reaction mixture was exposed to the following microwave irradiation protocol: (i) 5 min at power 30 and (ii) 10 min at power 10. The total reaction time was 15 min. The crude reaction solution was diluted in water (1:2) and dialyzed against distilled water for 4 d with frequent exchanges of the dialysis medium to remove unreacted Glu and its oligomeric side-products. Then, the solution was filtered (Filter Discs Qual., Grade 289, Sartorius AG, Goettingen, Germany), frozen at −20 °C (24 h) and freeze-dried (Lyophilizer L05, F.i.c, Scientific Instrumental Manufacturing, Buenos Aires, Argentina) at a condenser temperature of −45 °C and 30 μbar pressure (48 h). The product was stored at −20 °C until use. The glucosylated F127 was named F127-O-Glu.

### 2.3. Characterization of F127-O-Glu

#### 2.3.1. Nuclear Magnetic Resonance Spectroscopy (NMR)

The conjugation of Glu was confirmed by $^1$H NMR and $^{13}$C NMR spectroscopy in 20% w/v DMSO-$d_6$ solutions containing tetramethylsilane as internal standard, at 25 °C (see above).

#### 2.3.2. Attenuated Total Reflectance/Fourier Transform-Infrared Spectroscopy (ATR/FT-IR)

F127-O-Glu was characterized by ATR/FT-IR spectroscopy using a Nicolet 380 ATR/FT-IR spectrometer (Avatar Combination Kit, Smart Multi-Bounce HATR with ZnSe crystal 45° reflectance, Thermo Scientific, Madison, WI, USA) in the range between 4 000 and 600 cm$^{-1}$ (32 scans, spectral resolution of 4 cm$^{-1}$). Pristine F127 was used as control. Solid samples were mounted on the ATR crystal-metal plate and spectra were obtained using the OMNIC 8 spectrum software (Thermo Scientific).

#### 2.3.3. Matrix-Assisted Laser Desorption/Ionization Time of Flight Mass Spectrometry (MALDI-TOF MS)

The molecular weight of pristine F127 and F127-O-Glu was determined by MALDI-TOF MS (AUTOFLEX® mass spectrometer, Bruker Daltonics, Inc., Billerica, MA, USA) equipped with a pulsed nitrogen laser, operating at a wavelength of 337 nm in linear and reflectron mode, extracting positive ions with an accelerating voltage of 25 000 V, grid voltage set and grid wire voltage of 95 and 0.005%, respectively, and a delay time of 350 ns. The detection system consisted of a Micro Plate Channel with high sensitivity and dynamic range. 2-(4-Hydroxyphenylazo)-benzoic acid (0.1 M in chloroform) was used as the matrix. Samples were prepared as previously reported.[44] Briefly, copolymers were initially dissolved in chloroform (5 mg · mL$^{-1}$) and NaCl solution (0.1 M in water, 1 μL) was added to aid cationization (sample solution). Sample and matrix solutions were mixed in a 1:1 (v/v) ratio, deposited (1 μL) onto the MALDI sample holder and slowly dried to allow matrix crystallization. MALDI-TOF MS spectra were recorded and the intensity represented as a function of the *m/z* in the range between 2 000 and 20 000 g · mol$^{-1}$ (Bruker Daltonics Flex Analysis software, Bruker Daltonics, Inc.).

#### 2.3.4. Differential Scanning Calorimetry (DSC)

The thermal behavior of F127 and F127-O-Glu was analyzed by DSC using a Q100 V9.5 Build 288 differential scanning calorimeter (Universal V4.2E TA Instruments, New Castle, DE, USA) fitted with a liquid nitrogen cooling system. Dry samples (2.3–2.5 mg) were sealed in 40 μL Al-crucible pans and subjected to three consecutive thermal treatments at a heating/cooling rate of 5 °C · min$^{-1}$ and under nitrogen atmosphere: (i) heating from 25 to 100 °C (first heating ramp), (ii) cooling from 100 to −30 °C (cooling ramp) and (iii) heating from −30 to 150 °C (second heating ramp). The crystallization ($T_c$) and the melting temperature ($T_m$) of PEO blocks and the enthalpy involved in each transition ($\Delta H_c$ and $\Delta H_m$) were calculated from the exothermic and endothermic peaks, respectively, registered during the cooling and the second heating ramps (see above).

#### 2.3.5. Critical Micellar Concentration (CMC)

CMC values of F127 and F127-O-Glu were determined in MilliQ water (Simplicity® Water Purification System, Millipore, Billerica, MA, USA; pH = 5.8) at 25 and 37 °C. Derived count rate (DCR) measurements were carried out by means of dynamic light scattering (DLS, Zetasizer Nano-ZS, Malvern Instruments, Malvern,



*Macromol. Biosci.* **2014,** DOI: 10.1002/mabi.201400235

UK) at scattering angle of 173°.[35,44,51] The Nano-ZS contains a 4 mW He–Ne laser operating at a wavelength of 633 nm, a digital correlator ZEN3600, and a Non-Invasive Back Scatter (NIBS®) technology. For the measurements, pristine and glucosylated copolymers were solubilized (10% w/v final concentration) in water at 4 °C, the solutions were filtered (0.22 μm, GE nitrocellulose mixed esters membrane, Osmonics Inc., Minnesota, MN, USA) and finally diluted to the final concentration (0.00125–10% w/v) with water. Then, samples were equilibrated at the corresponding temperature for at least 24 h and analyzed by DLS. Refractive indices used for these measurements were between 1.333 and 1.350. Viscosities ranged between 0.8855–0.8890 cP at 25 °C and 0.6855–0.6873 cP at 37 °C. The intensity of the scattered light (DCR) expressed in kilo counts per second (kcps) was plotted as a function of the copolymer concentration (% w/v). Data for each single specimen was the result of at least five runs. The micellization was observed as a sharp increase in the scattering intensity. The intersection between the two straight lines corresponded to the CMC.[35,44,51]

## 2.4. Characterization of Drug-Free Micelles

### 2.4.1. Dynamic Light Scattering (DLS)

The hydrodynamic diameter ($D_h$), the size distribution (polydispersity index, PDI) and zeta potential (Z-potential) of F127 and F127-O-Glu PMs (10% w/v) freshly prepared in water and filtered (0.45 μm, white nitrocellulose membrane, Osmonics, Inc.) were measured using a Zetasizer Nano-ZS (see above), at 25 and 37 °C. The refractive index used for these measurements was 1.350 and the viscosity 0.8890 and 0.6873 cP at 25 and 37 °C, respectively. Results are expressed as mean ± SD of three independent samples prepared under identical conditions. Data for each single specimen was the result of at least six runs.

### 2.4.2. Nanoparticle Tracking Analysis (NTA)

The total concentration of F127 and F127-O-Glu polymeric micelles per mL freshly prepared in deionised water (1% w/v, stock solution, HPLC Grade, Rathburn Chemicals, Walkerburn, UK) was measured by means of Nanoparticle Tracking Analysis (NTA),[52,53] using a NS500-Zeta HSB system (NS500 instrument platform with high sensitivity camera and blue laser; NanoSight Ltd., Minton Park, UK), at 18, 24, and 37 °C. Results are expressed as mean ± S.D. of three independent samples prepared under identical conditions.

### 2.4.3. Transmission Electron Microscopy (TEM)

The morphology of freshly prepared F127 and F127-O-Glu PMs in water (see above) was visualized using a transmission electron microscope (Electron microscope ZEISS EM109 TEM, Oberkochen, Germany) equipped with a Digital ES1000W Erlangshen™ 11 megapixel high-speed affordable CCD camera (Model 785, Gatan GmbH, München, Germany). Samples (10% w/v, 50 μL) were pre-stabilized at 37 °C for at least 1 h and deposited onto a carbon grid membrane coated with a hydrophilic acrylic resin and incubated during 1 h at 37 °C prior to the analysis. After incubation, the excess of sample was soaked with filter paper and the grid covered with a drop of phosphotungstic acid (PTA; 50 μL, 2% w/v in deionized water, pH 7.0–7.5) during 60 s. Then, grids were air-dried and analyzed. The diameter of the micelles was estimated using the TEM AutoTune™ software (Gatan Digital Micrograph® software, Gatan GmbH). The analysis was done at 80 kV at room temperature.

## 2.5. Agglutination Assays

The binding affinity of F127-O-Glu polymeric micelles to the water-soluble vegetal lectin Concanavalin A (Con A, from *Canavalia ensiformis*, Jack Bean Type VI, lyophilized powder, Sigma–Aldrich) was initially evaluated by DLS, as reported elsewhere.[18,44] Briefly, pristine and modified PMs (20% w/v in PBS, pH = 7.2, 500 μL) containing bovine serum albumin (BSA, 6% w/v, Type V, Sigma–Aldrich) were incubated (30 min) at 25 °C, under continuous stirring. Then, Con A stock solution (1.0 mg · mL$^{-1}$ in PBS, pH = 7.2) was added (500 μL) to the micelles; the final concentrations of PMs, BSA and Con A in the sample were 10% w/v, 3% w/v, and 0.5 mg · mL$^{-1}$, respectively. Samples were incubated under moderate stirring at 37 °C for 2 h and the $D_h$ and the PDI monitored by DLS at the same temperature. The following controls were also analyzed: (i) BSA, (ii) BSA + Con A and (iii) pristine F127 PMs + BSA + Con A. Results are expressed as mean ± SD of three independent samples prepared under identical conditions. Data for each single specimen was the result of at least six runs. The agglutination was also characterized by UV spectrophotometry (λ = 215 nm, CARY [1E] UV-Visible Spectrophotometer, Varian, Inc., Lake Forest, CA, USA) where the absorbance of the samples was monitored over time. Finally, these assays were complemented with TEM analysis.[54,55] For this, PMs incubated with Con A under moderate stirring (2 h, 37 °C) were pre-stabilized (1 h, 37 °C) and visualized (see above). BSA + Con A and pristine F127 PMs + BSA + Con A were used as controls.

## 2.6. Preparation of DRV-Loaded PMs

To produce PMs, the required amount of copolymer was solubilized in water at 4 °C and then the solution was equilibrated at 25 °C at least 24 h before use. To screen the encapsulation capacity of pristine and modified PMs, DRV (in excess, ≈25 mg · mL$^{-1}$ copolymer solution) was added to 10% w/v F127 and F127-O-Glu PMs (5 mL) in caramel glass vials and sealed with paraffin film. Specimens were stirred (72 h) at 25 °C to enable the incorporation of DRV into the micelles and the resulting suspensions were filtered through clarifying filters (0.45 μm, white nitrocellulose membrane, Osmonics, Inc.) to remove insoluble drug. The drug payload in the different systems was quantified by UV spectrophotometry (λ = 267 nm, CARY [1E] UV–Visible Spectrophotometer) at room temperature, after the appropriate dilution in DMF. A calibration curve of DRV in DMF covering the range between 3.125 and 50 μg · mL$^{-1}$ ($R^2 > 0.999$) was used. DRV concentrations are expressed in μg · mL$^{-1}$ or mg · mL$^{-1}$. Solubility factors were calculated according to Equation (1)

$$f_s = S_{PM}/S_{water} \quad (1)$$



Macromol. Biosci. 2014, DOI: 10.1002/mabi.201400235

where $S_{PM}$ and $S_{water}$ are the apparent solubility of DRV in the corresponding micelles and the experimental intrinsic solubility in MilliQ water as determined in our laboratory (91 $\mu g \cdot mL^{-1}$ at 25 °C), respectively.

The size and size distribution of DRV-loaded micelles was analyzed by DLS (see above).

### 2.7. Statistical Analysis

The statistical analysis was performed by a one-way ANOVA combined with the Dunnett Multiple Comparison test or *t*-test; *p*-values smaller than 0.05 were considered statistically significant. The software used was GraphPad Prism version 5.00 for Windows (GraphPad Software, Inc., San Diego, CA, USA).

## 3. Results and Discussion

The decoration of the surface of PMs with sugar moieties has attracted our interest as a strategy to target hydrophobic drugs to cells expressing LLRs, especially macrophages.[18] However, time-consuming synthetic pathways, conjugation extents far from optimal and relatively low yields jeopardize the scale up and the technology transfer.[44,56] In this context, the present work investigated a simple, fast, and efficient microwave-assisted synthetic method for the production of glucose-conjugated PEO–PPOs and fully characterized the properties of the novel conjugate.

### 3.1. Microwave-Assisted Glucosylation of PEO–PPO

The conjugation of Glu to the terminal —OH groups of F127 was achieved by the ring opening of the sugar lactone in the presence of a biocompatible catalyst. To achieve a 100% conjugation, a F127:Glu molar ratio of 1:2 (with 10% molar excess of the sugar derivative) was used (Figure 1). Ring opening polymerizations are commonly used to synthesize polyesters and they were also introduced to produce synthetic homopolysaccharides with reasonably good yield of 75%.[57] Profuse literature has confirmed the advantage of microwave radiation to improve the performance of this type of reaction.[47–49] After dialysis and lyophilization, the F127-O-Glu product was a fine white powder and the yield was ≈90%.

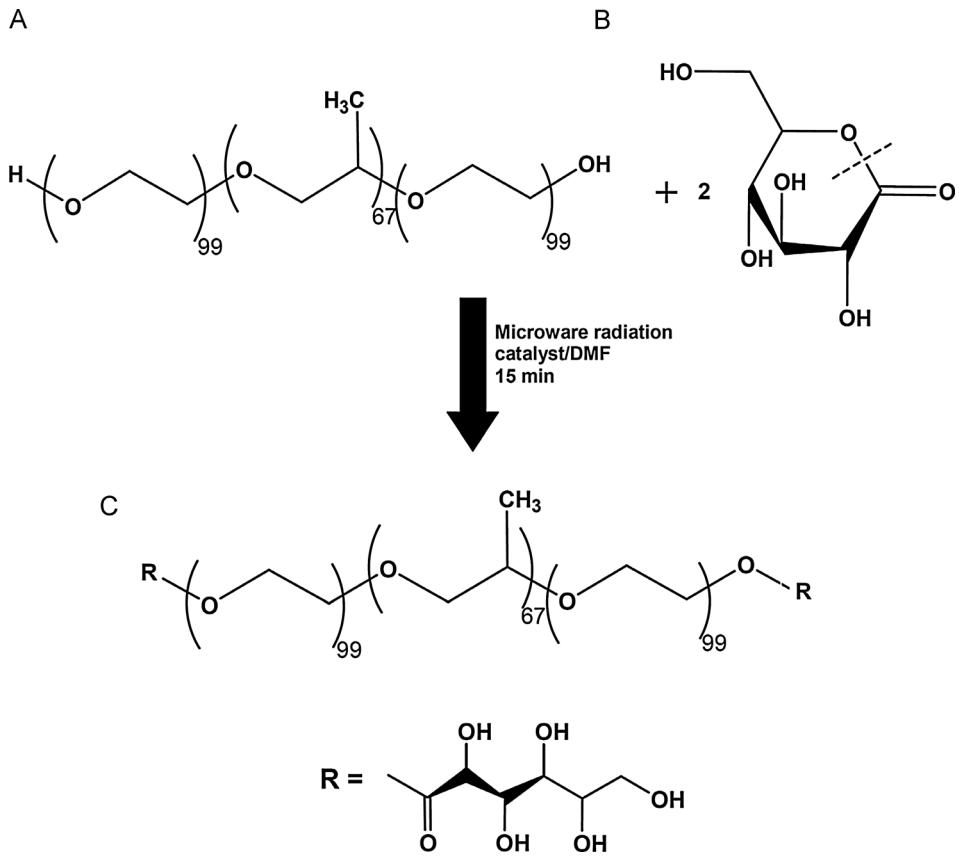


*Figure 1.* Synthetic pathway of the microwave-assisted ring opening conjugation of gluconolactone (B) to the terminal —OH of F127 (A), to render the F127-O-Glu derivative (C).

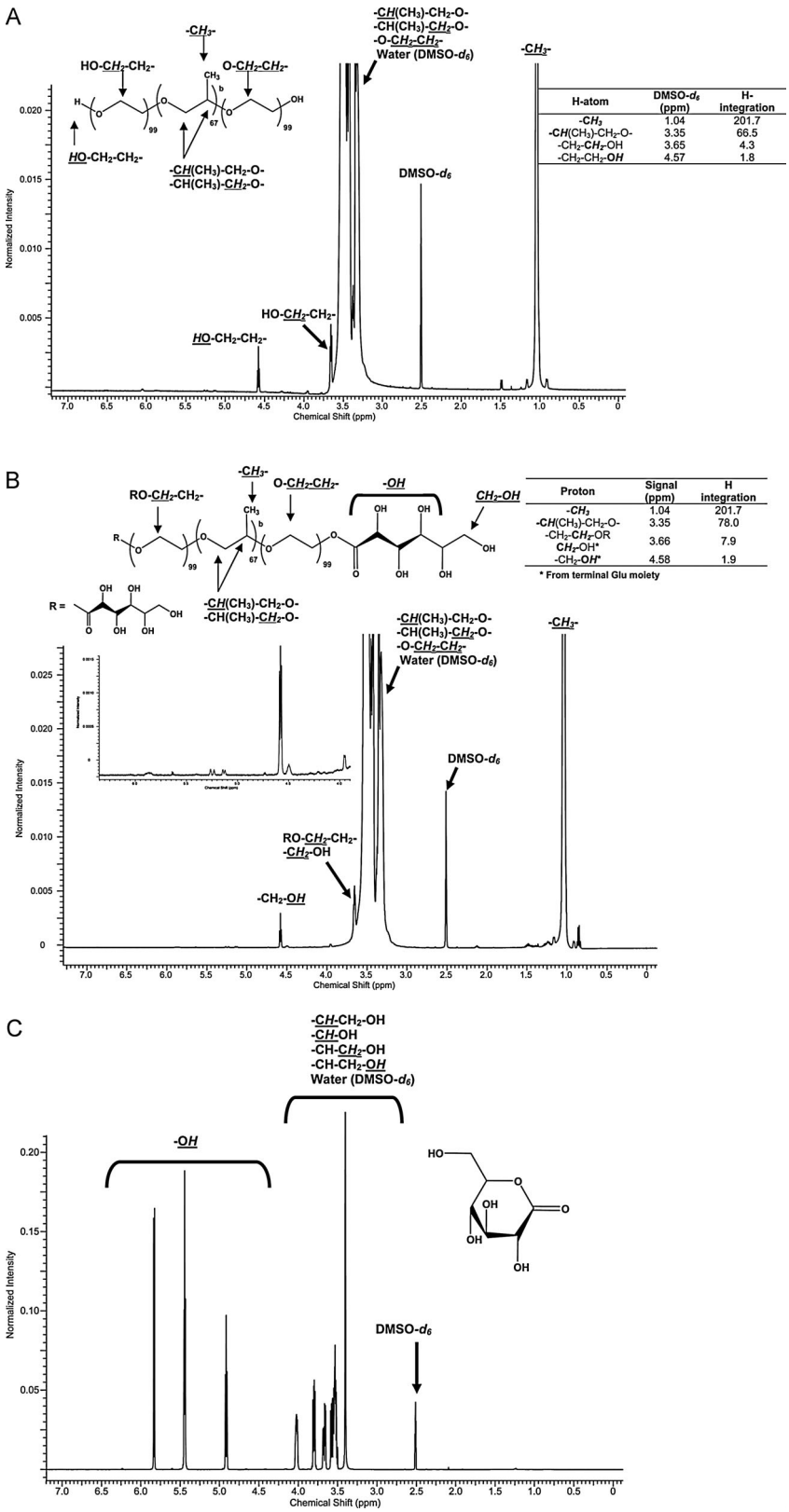


*Figure 2.* $^{1}$H NMR spectra of (A) pristine F127, (B) F127-O-Glu, and (C) pure gluconolactone in DMSO-$d_6$ with the assignment of the corresponding main proton signals. The *inset* in (B) shows a strong —$CH_2$—***OH*** triplet signal at 4.58 ppm and weak —*OH* signals (between 5.12 and 5.86 ppm) that correspond to the Glu moiety. The signal of —*OH* of pure gluconolactone appears between 4.85 and 5.75 ppm.



Macromolecular Journals

*Macromol. Biosci.* **2014,** DOI: 10.1002/mabi.201400235

### 3.2. Characterization of F127-O-Glu

The structure of F127-O-Glu was characterized by $^{1}$H NMR and $^{13}$C NMR and compared to that of F127 and Glu precursors. The characteristic protons of PPO (—C*H*$_3$) and PEO —(C*H*$_2$—C*H*$_2$)— in the pristine F127[58] and F127-O-Glu copolymers were observed at 0.90–1.20 and 3.40–3.70 ppm, respectively (Figure 2A and B). In addition, pristine F127 displayed a strong signal at 4.57 ppm integrating for two protons that corresponded to the two terminal —CH$_2$—*OH* groups (Figure 2A). It is important to mention that this signal was evident only in the dialyzed product, being almost unresolved in the non-dialyzed one that showed a very broad signal at approximately 4.6 ppm. Moreover, a Heteronuclear Single Quantum Coherence (HSQC) study revealed that these two protons belong to the terminal hydroxyl group (—*OH*) of pristine F127, as they did not correlate to any carbon atom of the copolymer (data not shown). Additionally, —*CH*$_3$, —*CH* and —CH$_2$—*CH*$_2$—OH integrated for 202, 67, and 4 hydrogens, at 1.04, 3.35, and 3.65 ppm, respectively (Figure 2A). These results were consistent with the number of PEO and PPO repeating units in F127 (see F127 structure in Figure 2A). F127-O-Glu presented a more complex spectrum combining the characteristic signals of F127 and the sugar: the terminal protons involved in the ester bond between the copolymer and the sugar (—C*H*$_2$—O-Glu) were observed as a strong triplet signal at 3.66 ppm beside the —*CH*$_2$—OH belonging to the terminal Glu moiety. In this case, the integration of the triplet signal corresponded to eight protons instead of four (as observed in the pristine copolymer). The terminal CH$_2$—*OH* of the Glu moiety slightly shifted to 4.58 ppm (1.16 Hz shift with respect to the terminal —OH of the pristine F127) (Figure 2B) and weak signals corresponding to the multiple hydroxyl groups of Glu (—*OH*) were observed between 5.12 and 5.86 ppm (Figure 2B, inset). These signals were in good agreement with those of Glu (Figure 2C). It is worth mentioning that, according to HSQC, the two protons at 4.58 ppm did not correlate with any carbon, as for the pristine F127 (data not shown). Thus, the signal was assigned to the hydroxyl groups of the sugar moieties (Figure 2B). In addition, the signal of —*CH* in Glu could overlap with those of the copolymer at ≈3.3–3.4 ppm (Figure 2B). This is also evidenced by the increase of the integration area of —*CH* protons at 3.36 ppm for F127-O-Glu with respect to the pristine copolymer (see assignment of the main protons in Figure 2A, B). This is another evidence of the addition of two molecules of Glu per molecule of F127. Finally, $^{13}$C NMR showed a very weak signal at 171.91 ppm that corresponded to the C=O of the conjugated gluconolactone (Figure S2). These results were in agreement with the literature.[59,60] At the same time, the reliable quantification of the modification extent by this technique was very difficult due to the labile nature of the protons of —OH groups and their small relative area compared to the protons of the copolymer. Thus, we analyzed the conjugate by MALDI-TOF MS (see below).

ATR/FT-IR was useful tool to confirm the successful modification of F127. The pristine copolymer showed the stretching vibration of C—H and C—O—C of PEO and PPO blocks at 2 890 and 1 111 cm$^{-1}$ (Figure 3A). In the case of F127-O-Glu, these bands were slightly shifted to 2 877 and 1 078 cm$^{-1}$ (Figure 3B). Moreover, the conjugate showed strong bands at 3 417 and 1 647 cm$^{-1}$ that corresponded to the stretching vibration of —OH and carbonyl groups of Glu, respectively (Figure 3B). Similar findings were reported by other authors for different natural and synthetic polymers modified with different sugar residues.[61,62]

To determine the molecular weight of F127-O-Glu, the material was analyzed by MALDI-TOF MS. The analysis of high molecular weight polymers by this technique is usually challenging due to the overlapping of signals belonging to several fragments.[63] On the other hand, the softness of the ionization conditions minimize fragmentation;[64] in positive mode, polyethoxylates are ionized by adduct formation with alkali metal ions, mostly sodium or potassium. Thus, in our work, maximum intensity peaks appeared as $[m/z + \mathrm{Na}]^+$ (g · mol$^{-1}$) due to the formation of Na alkoxides in the terminal —OH groups of fragmented PEO–PPO copolymers.[44,63] Pristine F127, showed two peaks that ranged between 2 370 and 6 864 g · mol$^{-1}$, with two maxima at $[m/z + \mathrm{Na}]^+$ 3 470 and 4 950 g · mol$^{-1}$.[44] These signals fitted quite well the theoretical molecular weight of PPO (3 886 g · mol$^{-1}$) and PEO (4 356 g · mol$^{-1}$) segments in this copolymer (Table 1). In this case, the signal of the non-fragmented molecule was not observed. Thus,

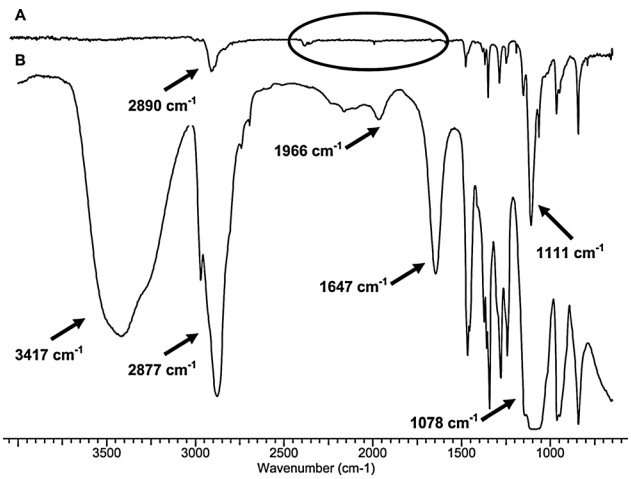


*Figure 3.* ATR/FT-IR spectrum of (A) pristine F127 and (B) F127-O-Glu derivative. Pristine F127 was dialyzed and lyophilized before the analysis.



*Macromol. Biosci.* **2014,** DOI: 10.1002/mabi.201400235

*Table 1.* Mean weight molecular mass ($\overline{M}_w$) fractions of pristine F127 and F127-O-Glu copolymers, as determined by MALDI-TOF MS. Values were corrected by the subtraction of two $Na^+$ ions (one per terminal —OH).

| Copolymer | Theoretical molecular weight [g · mol$^{-1}$] | $[m/z + Na]^+_1$ [g · mol$^{-1}$] PPO | $[m/z + Na]^+_2$ [g · mol$^{-1}$] PEO | Experimental molecular weight [g · mol$^{-1}$][c)] |
|---|---|---|---|---|
| F127 | 12 600[a)] | 3 470 | 4 950 | 13 240 |
| F127-O-Glu | 12 960[b)] | 3 080 | 5 360 | 13 660 |

[a)]Value provided by the supplier; [b)]Value calculated by the addition of two Glu molecules to the molecular weight of the pristine copolymer; [c)]Experimental molecular weights were calculated by the sum of one $[m/z + Na]^+_1$ and two $[m/z + Na]^+_2$, adjusted by the subtraction of the corresponding $Na^+$ ions of each terminal —OH group.

the molecular weight calculated from the sum of the molecular weights of two PEO and one PPO fragments, where each value adjusted after the subtraction of two $Na^+$ ions (46 g · mol$^{-1}$). The value was 13 240 g · mol$^{-1}$, being in good agreement with the accepted average molecular weight of pristine F127 (12 600 g · mol$^{-1}$). At the same time, it should be stressed that small to intermediate deviations from the theoretical values have been previously reported for PEO–PPOs.[33] The distribution of F127-O-Glu was similar to that of the unmodified copolymer, with $[m/z + Na]^+$ values ranging between 2 283 and 6 909 g · mol$^{-1}$ and two maxima at 3 080 and 5 360 g · mol$^{-1}$ (Figure 4, Table 1).

The calculation of the molecular weight following the same procedure used for pristine F127 resulted in a value of 13 660 g · mol$^{-1}$. Furthermore, the spectrum showed a third small fraction of $[m/z + Na]^+$ 13 708 g · mol$^{-1}$ that, after subtraction of two $Na^+$ ions, corresponded to a non-fragmented molecule with a molecular weight of 13 660 g · mol$^{-1}$, in full agreement with the molecular weight calculated by the sum of the different segments (Figure 4, Table 1). This result strongly suggests that the glucosylation slightly increased the stability of the molecule to ionization, reducing the fragmentation phenomenon, probably due to the end-capping of the terminal —OH groups. The increase of the molecular weight from the pristine to the modified copolymer (420 g · mol$^{-1}$) was in good agreement with the addition of two Glu molecules per F127 triblock, indicating a 100% modification extent (Table 1). These findings are very promising considering that the reaction demanded only 15 min and the yield was almost optimal.

To assess the effect of Glu conjugation on the thermal behavior of PEO segments in the copolymer, the pristine and the modified copolymer were analyzed by DSC; PPO is a fully amorphous component. Initially, samples were heated from room temperature to 100 °C to erase the thermal history and then they were exposed to a cooling/heating cycle. The $T_c$ was evidenced as a sharp exothermic peak at 31.2 °C for F127[44] and 33.2 °C for F127-O-Glu (Table 2).

In addition, the $T_m$ was visualized as broad endothermic peaks at 54.7 and 56.4 °C, for the pristine and the modified copolymer, respectively. The enthalpies involved in the crystallization and the melting were very similar; e.g., $\Delta H_c$ and $\Delta H_m$ of F127 were 133.8 and 134.6 J · g$^{-1}$, respectively. On the other hand, regardless of the slight changes in the temperature of both transitions, $\Delta H_c$ and $\Delta H_m$ values for F127-O-Glu were approximately five times smaller than those of the pristine copolymer (Table 2), suggesting that the sugar residues hindered the crystallization of PEO

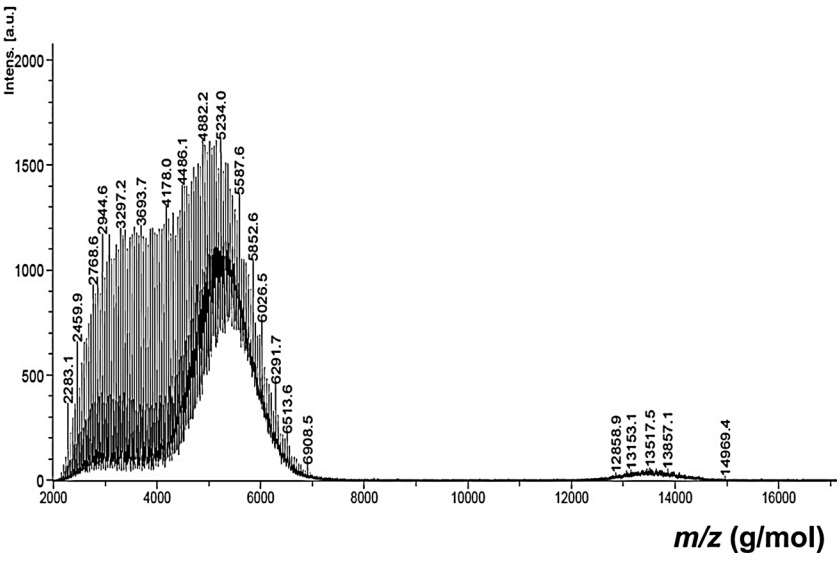


*Figure 4.* MALDI-TOF spectrum of F127-O-Glu.



Macromol. Biosci. 2014, DOI: 10.1002/mabi.201400235

*Table 2.* DSC data of pristine F127 and F127-O-Glu copolymers.

| Copolymer | $T_c$ [a)] [°C] | $\Delta H_c$ [a)] [J · g$^{-1}$] | $T_m$ [b)] [°C] | $\Delta H_m$ [b)] [J · g$^{-1}$] |
|---|---|---|---|---|
| F127 | 31.2 | 133.8 | 54.7 | 134.6 |
| F127-O-Glu | 33.2 | 27.1 | 56.4 | 26.5 |

[a)]Determined during the cooling ramp; [b)]Determined during the second heating ramp.

*Table 3.* Experimental CMC values of pristine F127 and F127-O-Glu in water (pH = 5.8) at 25 and 37 °C, as determined by DLS.

| | Water [% w/v] | |
|---|---|---|
| Copolymer | 25 °C | 37 °C |
| F127 | 0.25 | 0.06 |
| F127-O-Glu | 0.02 | 0.01 |

segments. These results constitute further evidence of the effective glucosylation.

The goal of the Glu modification to the PEO–PPO copolymer was to confer active targeting capacity to the PMs. However, the conjugation could affect the self-aggregation phenomenon and the physical stability of the micelles in aqueous medium. To assess the effect of Glu residues on the micellization process, we determined the CMC of both amphiphiles under the same conditions. At 25 °C, pristine F127 showed a CMC value of 0.25% w/v (Table 3). The increase of the temperature to 37 °C resulted in a sharp decrease of the CMC to 0.06% w/v that was consistent with the reverse thermo-responsiveness of PEO–PPOs.[44,65,66] F127-O-Glu showed remarkably smaller values of 0.02 and 0.01% w/v at 25 and 37 °C, respectively. These findings suggested that the conjugation of glucose residues increase the micellization tendency by means of the physical stabilization of the micelle by hydrogen bonding in the corona (Table 3), as shown elsewhere for lactosylated derivatives.[44] This is a very beneficial feature that would improve the drug encapsulation capacity of the micelles. It is worth mentioning that a reduction of the CMC would have biological implications owing to the expected greater stability of the aggregates under extreme dilution conditions such as those undergone after intravenous or oral administration.

### 3.3. Characterization of F127-O-Glu Micelles

The size, size distribution and surface charge density are features that govern the physical stability, the drug encapsulation capacity and the interaction of the micelles with cells. Initially, the analysis was conducted by DLS. Regardless of the temperature, F127 showed a monomodal size distribution and micelles shrank upon heating from 53.2 to 25.8 nm (Table 4). This behaviour was consistent with the thermo-responsive nature of these copolymers.[44,67]

The conjugate showed a different aggregation pattern that combined a minor population (23–26%) of relatively small-size micelles ($D_h$ being 40.7 nm at 25 °C and 21.6 nm at 37 °C) and a major one (74–77%) with substantially larger sizes of 415.2 and 227.9 nm at 25 and 37 °C, respectively (Table 4). The PDI increased in accordance from 0.30–0.36 for the unmodified to 0.53–0.66 for the modified copolymer. These results were consistent with those observed with lactosylated PEO–PPOs[44] and would suggest the secondary aggregation of the micelles probably due to the interaction of sugar moieties of different micelles. The Z-potential of the micelles at both temperatures was almost neutral, with a very slight twist from negative to positive values upon heating (Table 4).

*Table 4.* Size ($D_h$), size distribution (PDI), Z-potential and electrophoretic mobility of 10% (w/v) F127 and F127-O-Glu micelles in water at 25 and 37 °C, as measured by DLS. F127 was dialyzed before analysis.

| | | Peak 1[a)] | | Peak 2[b)] | | | |
|---|---|---|---|---|---|---|---|
| Copolymer | $T$ [°C] | $D_h$ [nm] (S.D) | % Intensity (S.D) | $D_h$ [nm] (S.D) | % Intensity (S.D) | PDI [S.D] | Z-potential [mV] [S.D] |
| F127 | 25 | 53.2 (2.3) | 100.0 (0.0) | – | – | 0.357 (0.038) | −4.25 (1.22) |
| F127-O-Glu | | 40.7 (4.0) | 25.6 (1.6) | 415.2 (29.9) | 74.4 (1.6) | 0.655 (0.017) | −1.96 (0.17) |
| F127 | 37 | 25.8 (4.2) | 100.0 (0.0) | – | – | 0.302 (0.088) | +1.57 (0.21) |
| F127-O-Glu | | 21.6 (1.6) | 22.6 (4.6) | 227.9 (54.1) | 77.4 (4.6) | 0.531 (0.167) | +1.06 (0.50) |

[a)]Size population of smaller size; [b)]Size population of larger size.

*Table 5.* Concentration of F127 and F127-O-Glu PMs per mL at 18, 24 and 37 °C, as measured by NTA.

| Temperature [°C] | Copolymer | Particle concentration [$10^8$/mL] (S.D) |
|---|---|---|
| 18 | F127 | 6.7 (0.9) |
| | F127-O-Glu | 4.6 (0.4) |
| 24 | F127 | 5.2 (0.2) |
| | F127-O-Glu | 4.5 (0.3) |
| 37 | F127 | 3.6 (0.3) |
| | F127-O-Glu | 2.8 (0.1) |

NTA is an innovative device that enables the quantification and visualization of nano and submicron particles.[52,53] This feature is extremely useful in pharmaceutical development because it can be used to quantify the drug cargo per particle. In general, for identical copolymer concentrations, F127 showed a greater number of micelles than F127-O-Glu; e.g., the number decreased from 6.7, 5.2 and $3.6 \times 10^8$ micelles/mL for F127 to 4.6, 4.5 and 2.8 for F127-O-Glu, at 18, 24 and 37 °C, respectively (Table 5).

Samples underwent 1000× dilution immediately before measurement to adjust the amount of particles per volume unit to the specifications of the equipment. Thus, these results would strongly suggest that the decrease in the number of micelles for the modified copolymer stemmed from a greater aggregation number and from a secondary aggregation phenomenon that is likely in more concentrated systems. The growth in the aggregation number was consistent with the larger size of F127-O-Glu micelles, as observed by DLS. In addition, the micellar concentration drop over heating indicated the more complete micellization of both copolymers and the formation of micelles of greater aggregation number, though smaller size due to their shrinkage at higher temperatures. Videos enabled the direct visualization of the micelles in suspension and showed the uniform Brownian motion (see Supplementary Videos).

The spherical morphology of F127 and F127-O-Glu micelles was confirmed by TEM (Figure 5). Sizes were larger than those determined by DLS, especially for pristine F127 (Figure 5A, Table 4). These findings suggest changes in the aggregation pattern during the sample preparation.

### 3.4. Concanavalin A Agglutination

The availability of sugar molecules on the surface of the polymeric micelles is a prerequisite to enable their interaction with LLRs and the active targeting of the encapsulated drug to a specific cell type. There exist fast and economic *in vitro* assays that employ soluble lectins to primarily assess the substrate-receptor interaction. In this framework, pristine F127 and F127-O-Glu polymeric micelles were incubated with Con A at 37 °C and the $D_h$ and the PDI were monitored over 2 h, by DLS.[18,44] This assay was complemented by measuring the absorbance of the samples by UV spectrophotometry. When pristine F127 micelles were incubated with Con A, no agglutination phenomenon was evident (Table 6). The sizes from 18.4 and 371.1 nm (with BSA and without Con A, respectively) changed to 13.9 and 321.2 nm (with BSA + Con A). In addition, the UV absorbance did not change significantly with a slight increase from 3.966 to 4.796. Furthermore, a Con A + BSA 3% control displayed an absorbance value of 3.428, being in the same order of the former two samples. It is important to stress that pristine F127 in water at 37 °C displayed a monomodal size distribution of 25.8 nm (Table 4). The appearance of a second population of larger size (321.2–371.1 nm, Table 6) due to the presence of BSA was in agreement with a non-specific agglutination phenomenon.

Conversely, when F127-O-Glu micelles were exposed to Con A, larger aggregates of approximately 1.7 μm were rapidly formed and the absorbance sharply increased from 4.440 to >10 (Table 6), confirming a specific agglutination phenomenon in presence of Con A. On the other hand, the presence of BSA (without Con A) in F127-O-Glu PMs increased the size of the second population from 227.9 to 576.3 nm (Tables 4 and 6) owing to non-specific

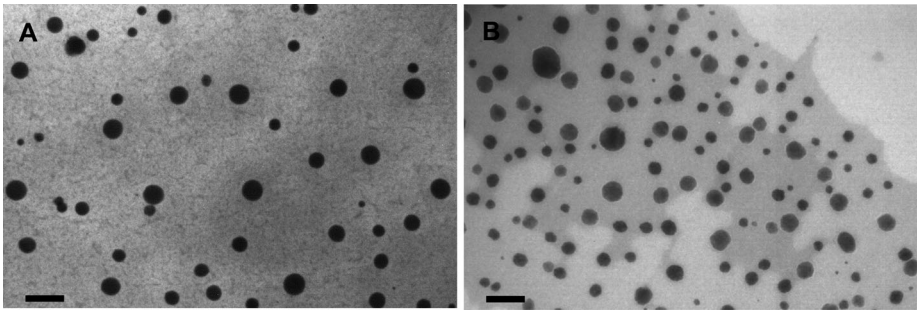


*Figure 5.* TEM micrographs of 10% w/v polymeric micelles. (A) Pristine F127 and (B) F127-O-Glu. Samples were stabilized at 37 °C for at least 1 h prior to the analysis. Scale bar: 500 nm.



Macromolecular Journals

*Macromol. Biosci.* **2014,** DOI: 10.1002/mabi.201400235

*Table 6.* Size ($D_h$) and size distribution (PDI) and absorbance of 10% (w/v) F127 and F127-O-Glu micelles after incubation with BSA 3% without and with Con A in PBS (pH 7.2) over 2 h at 37 °C, as measured by DLS.

| | | Peak 1[a)] | | Peak 2[b)] | | | |
|---|---|---|---|---|---|---|---|
| Copolymer | Con A [mg · mL$^{-1}$] | $D_h$ [nm] (S.D) | % Intensity (S.D) | $D_h$ [nm] (S.D) | % Intensity (S.D) | PDI (S.D) | Absorbance[d)] |
| F127 | 0 | 18.4 (0.5) | 79.5 (1.1) | 371.1 (30.2) | 20.5 (1.1) | 0.299 (0.081) | 3.966 |
| | 0.5 | 13.9 (0.5) | 79.6 (2.0) | 321.2 (60.6) | 20.4 (2.0) | 0.335 (0.031) | 4.796 |
| F127-O-Glu | 0 | 21.7 (0.3) | 69.9 (0.9) | 576.3 (82.1) | 30.1 (0.9) | 0.479 (0.058) | 4.440 |
| | 0.5 | 17.0 (0.2) | 71.0 (3.1) | 1682[c)] (379.7) | 29.0 (3.1) | 0.323 (0.092) | >10 |

[a)]Size population of smaller size; [b)]Size population of larger size; [c)]Statistically significant increases in size when compared to the non-modified copolymer treated with Con A ($p < 0.05$). [d)]Measured at 215 nm.

aggregation, as it was apparent for pristine F127 (see above). The agglutination process was visualized by TEM where the Con A led to the gradual fusion of the micelles of F127-O-Glu to form large aggregates that lost their original spherical shape (Figure 6B), as opposed to pristine F127 PMs that showed the non-specific aggregation observed by DLS (Figure 6A). Overall, these results strongly suggested the conservation of unmodified hydroxyl groups in C3, C4 and C6 that is fundamental for the binding to the lectin.[68,69] At the same time, it should be mentioned that in some cases, the partial modification of these residues does not completely inhibit the binding capacity owing to the availability of secondary binding sites in the protein.[44,70]

### 3.5. Encapsulation of DRV within Polymeric Micelles

DRV is a non-peptidic protease inhibitor (PI) (Figure S1A) of the human immunodeficiency virus type 1 (HIV-1) indicated for the treatment infected adults and children above the 3 years of age.[71,72] The absolute oral bioavailability of a single DRV dose (600 mg) alone and after co-administration with the boosting agent ritonavir (RTV, 100 mg) is 37% and 82%, respectively.[71] While DRV/RTV is a highly effective combination, it is only used as a second-line option in high-income countries; World Health Organization guidelines do not recommend boosted DRV as first-line due to high cost and unavailability of a heat-stable fixed-dose combination.[72] Encapsulation of DRV could improve its aqueous solubility and oral bioavailability and reduce the required dose (and the cost) and thus, make this medication more affordable.[73–75] In this scenario, we assessed for the first time the encapsulation of DRV within a polymeric nanocarrier. 10% w/v pristine F127 and F127-O-Glu PMs increased the solubility of DRV from 91 μg · mL$^{-1}$ to 14.2 ($f_s = 156$) and 18.9 mg · mL$^{-1}$ ($f_s = 209$), respectively (Table 7). The increase in the encapsulation capacity for the glucosylated derivative was associated with the sharp decrease of its CMC (Table 3).

The size is a critical parameter that governs the physical stability of the dispersions and the interaction of the drug-loaded nanocarriers with cells and tissues and it can also condition the absorption process in mucosa.[45] In this context, the size and size distribution of the different unmodified and glucosylated DRV-loaded PMs were

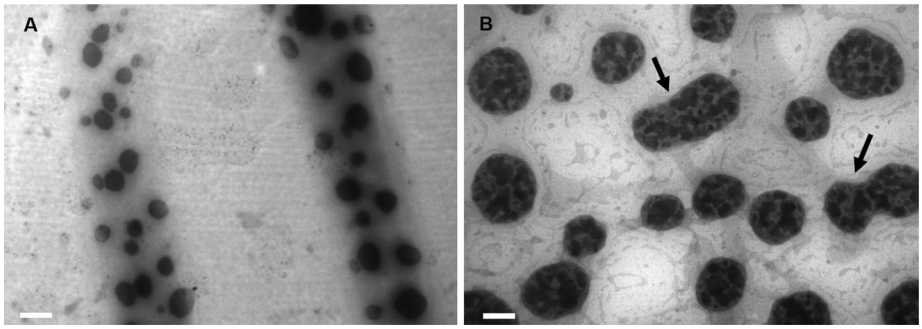


*Figure 6.* TEM micrographs of 10% w/v polymeric micelles incubated with Con A + BSA at 37 °C. (A) Pristine F127 and (B) F127-O-Glu. Samples were stabilized at 37 °C for at least 1 h prior to the staining. The fusion of F127-O-Glu and the formation of non-spherical aggregates are pointed out with arrows in B. Scale bar: 200 nm.

*Table 7.* Drug-loading, solubility factor, size ($D_h$) and size distribution (PDI) of DRV-loaded 10% (w/v) F127 and F127-O-Glu micelles at 25 and 37 °C, as measured by DLS.

| | | | | Peak 1[a)] | | Peak 2[b)] | | |
|---|---|---|---|---|---|---|---|---|
| Copolymer [10% w/v] | DRV load [mg · mL$^{-1}$] (S.D) | Solubility factor ($f_s$) | $T$ [°C] | $D_h$ [nm] (S.D) | % Intensity (S.D) | $D_h$ [nm] (S.D) | % Intensity (S.D) | PDI (S.D) |
| F127 | 14.2 (3.4) | 156 | 25 | – | – | 1402.0 (99.3) | 100.0 (0.0) | 0.071 (0.071) |
| | | | 37 | 20.5 (0.4) | 59.4 (2.7) | 436.9 (19.3) | 40.6 (2.7) | 0.620 (0.031) |
| F127-O-Glu | 18.9 (3.7) | 209 | 25 | – | – | 1364.0 (99.1) | 100.0 (0.0) | 0.064 (0.038) |
| | | | 37 | 24.7 (0.9) | 83.0 (3.0) | 744.7 (160.9) | 17.0 (3.0) | 0.358 (0.050) |

[a)]Size population of smaller size; [b)]Size population of larger size.

characterized by DLS at 25 and 37 °C. At 25 °C, the pristine and modified PMs displayed a monomodal distribution with large structures of 1 402 and 1364 nm, respectively, and relatively small PDI values <0.071 (Table 7). These findings suggested that drug-loaded micelles probably underwent secondary aggregation to stabilize the system.[76] Conversely, at 37 °C, both drug-loaded PMs shrank and displayed a bimodal aggregation pattern with sizes that were larger than those of the unloaded systems (Table 7). These results indicated that, under these conditions, the drug led to the enlargement of the micelle. Finally, drug concentrations and hydrodynamic sizes remained constant for at least 24 h at 30 °C (data not shown).

## 4. Conclusion

In this work, we investigated a fast, efficient and reproducible synthetic pathway for the glucosylation of polymeric amphiphiles towards the production of PMs that are recognizable by lectins. A high conjugation extent of approximately 100% was achieved in a relatively short time and with very high yield. The conjugation of Glu moieties favored the micellization process, as expressed by the lower CMC values measured. Con A experiments *in vitro* support the potential of this scalable nanotechnology to target drugs to cells expressing LLRs. Finally, this behavior favored the encapsulation of the antiretroviral DRV and open new possibilities to develop innovative products with improved biopharmaceutical performance.

Acknowledgement: RJG is staff member of CONICET. The work was supported by grant of CONICET (PIP0220). The authors are very thankful to Dr. Omar Sued (Fundacion Huesped, Buenos Aires, Argentina) for valuable discussions and inputs on the clinical challenges faced in HIV. We also thank Prof. Dr. Carmen Alvarez-Lorenzo (Department of Pharmacy and Pharmaceutical Technology, Universidad de Santiago de Compostela, Spain), Prof. Dr. Viviana Campo Campo Dall'Orto (Department of Analytical Chemistry, Faculty of Pharmacy and Biochemistry, University of Buenos Aires, Argentina) and Dr. Ellie Lanning and Joanna Sullivan (NanoSight® Ltd.) for DSC and MALDI-TOF, ATR/FT-IR and NTA analyses, respectively. AS thanks the European Union's - Seventh Framework Programme under grant agreement #612675-MC-NANOTAR.

Received: May 14, 2014; Revised: July 30, 2014; Published online: DOI: 10.1002/mabi.201400235

Keywords: darunavir free base; gluconolactone; Glucosylated poly(ethylene oxide)-*b*-poly(propylene oxide) block copolymers; microwave-assisted ring opening conjugation; polymeric micelles

[1] C. F. Nathan, *J. Clin. Invest.* **1987**, *79*, 319.
[2] Y. R. Mahida, *Inflamm. Bowel. Dis.* **2000**, *6*, 21.
[3] J. L. Flynn, J. Chan, *Infect. Immun.* **2001**, *69*, 4195.
[4] S. Koening, H. E. Gendelman, J. M. Orenstein, M. C. Dal Canto, G. H. Pezeshkpour, M. Yungbluth, F. Janotta, A. Aksamit, M. A. Martin, A. S. Fauci, *Science* **1986**, *233*, 1089.
[5] F. Chappuis, S. Sundar, A. Hailu, H. Ghalib, S. Rijal, R. W. Peeling, J. Alvar, M. Boelaert, *Nat. Rev. Microbiol.* **2007**, S7–S16.
[6] A. N. Zelensky, J. E. Gready, *FEBS J.* **2005**, *272*, 6179.
[7] R. T. Lee, T. L. Hsu, S. K. Huang, S. L. Hsieh, C. H. Wong, Y. C. Lee, *Glycobiology* **2011**, *21*, 512.
[8] S.-H. Kim, M. Goto, T. Akaike, *J. Biol. Chem.* **2001**, *276*, 35312.
[9] K. C. Carvalho, I. W. Cunha, R. M. Rocha, F. R. Ayala, M. M. Cajaíba, M. D. Begnami, R. S. Vilela, G. R. Paiva, R. G. Andrade, F. A. Soares, *Clinics* **2011**, *66*, 965.
[10] A. M. Kerrigan, G. D. Brown, *Immunobiology* **2009**, *214*, 562.
[11] H. Sheikh, H. Yarwood, A. Ashworth, C. M. Isacke, *J. Cell. Sci.* **2000**, *113*, 1021.
[12] S. Burgdorf, V. Lukacs-Kornek, C. Kurts, *J. Immunol.* **2006**, *176*, 6770.
[13] C. A. Janeway, P. Travers, M. Walport, M. J. Shlomchik, In "*Immunobiology: The Immune System in Health and Disease*", 5th edition, Garland Science, New York **2001**.
[14] Y. Han, L. Zhao, Z. Yu, J. Feng, Q. Yu, *Int. Immunopharmacol.* **2005**, *5*, 1533.
[15] H.-L. Jiang, M.-L. Kang, J.-S. Quan, S.-G. Kang, T. Akaike, H. S. Yoo, *Biomaterials* **2008**, *29*, 1931.

[16] J. M. Irache, H. H. Salman, C. Gamazo, S. Espuelas, *Expert Opin. Drug Deliv.* **2008**, *5*, 703.
[17] R. Duncan, *Nat. Rev. Cancer* **2006**, *6*, 688.
[18] M. A. Moretton, D. A. Chiappetta, F. Andrade, J. das Neves, D. Ferreira, B. Sarmento, A. Sosnik, *J. Biomed. Nanotechnol.* **2013**, *9*, 1076.
[19] K. N. Jain, V. Mishra, N. K. Mehra, *Expert Opin. Drug Del.* **2013**, *10*, 353.
[20] K. Kataoka, A. Harada, Y. Nagasaki, *Adv. Drug Del. Rev.* **2001**, *47*, 113.
[21] A. Sosnik, In Smart Materials for Drug Delivery. C. Alvarez-Lorenzo, A. Concheiro, Eds., "*Royal Society of Chemistry*", London **2013**, Chapter 5 pp. 115.
[22] C. Alvarez-Lorenzo, A. Sosnik, A. Concheiro, *Curr. Drug Targets* **2011**, *12*, 1112.
[23] L. Bromberg, *J. Control. Release* **2008**, *128*, 99.
[24] X.-B. Xiong, Z. Binkhathlan, O. Molavi, A. Lavasanifar, *Acta Biomater.* **2012**, *8*, 2017.
[25] G. Gaucher, P. Satturwar, M.-C. Jones, A. Furtos, J.-C. Leroux, *Eur. J. Pharm. Biopharm.* **2010**, *76*, 147.
[26] A. Sosnik, A. Carcaboso, D. A. Chiappetta, *Recent Pat. Biomed. Eng.* **2008**, *1*, 43.
[27] D. A. Chiappetta, A. Sosnik, *Eur. J. Pharm. Biopharm.* **2007**, *66*, 303.
[28] E. V. Batrakova, A. V. Kabanov, *J. Control. Release* **2008**, *130*, 98 Pluronic Block Copolymers.
[29] J. Gonzalez-Lopez, C. Alvarez-Lorenzo, P. Taboada, A. Sosnik, I. Sandez-Macho, A. Concheiro, *Langmuir* **2008**, *24*, 10688.
[30] D. A. Chiappetta, J. Degrossi, S. Teves, M. D'Aquino, C. Bregni, A. Sosnik, *Eur. J. Pharm. Biopharm.* **2008**, *69*, 535.
[31] R. N. Peroni, S. S. Di Gennaro, C. Hocht, D. A. Chiappetta, M. C. Rubio, A. Sosnik, G. F. Bramuglia, *Biochem. Pharmacol.* **2011**, *82*, 1227.
[32] D. A. Chiappetta, C. Hocht, C. Taira, A. Sosnik, *Nanomedicine (Lond.)* **2010**, *5*, 11.
[33] D. A. Chiappetta, C. Alvarez-Lorenzo, A. Rey-Rico, P. Taboada, A. Concheiro, A. Sosnik, *Eur. J. Pharm. Biopharm.* **2010**, *76*, 24.
[34] D. A. Chiappetta, C. Hocht, C. Taira, A. Sosnik, *Biomaterials* **2011**, *32*, 2379.
[35] D. A. Chiappetta, G. Facorro, E. Rubin de Celis, A. Sosnik, *Nanomed.: Nanotechnol. Biol. Med.* **2011**, *7*, 624.
[36] A. Ribeiro, A. Sosnik, D. A. Chiappetta, F. Veiga, A. Concheiro, C. Alvarez-Lorenzo, *J. R. Soc. Interface* **2012**, *9*, 2059.
[37] C. Garcia Vior, J. Marino, L. P. Roguin, A. Sosnik, J. Awruch, *Photochem. Photobiol.* **2013**, *89*, 492.
[38] D. A. Chiappetta, C. Hocht, J. A. W. Opezzo, A. Sosnik, *Nanomedicine (Lond.)* **2013**, *8*, 223.
[39] C. Alvarez-Lorenzo, A. Rey-Rico, J. Brea, M. I. Loza, A. Concheiro, A. Sosnik, *Nanomedicine (Lond.)* **2010**, *5*, 1371.
[40] M. L. Cuestas, A. Sosnik, V. L. Mathet, *Mol. Pharmaceutics* **2011**, *8*, 1152.
[41] M. L. Cuestas, A. Castillo, A. Sosnik, V. L. Mathet, *Bioorg. Med. Chem. Lett.* **2012**, *22*, 6577.
[42] A. Sosnik, *Adv. Drug Deliv. Rev.* **2013**, *65*, 1828.
[43] C. R. Becer, *Macromol. Rapid Commun.* **2012**, *33*, 742.
[44] M. L. Cuestas, R. J. Glisoni, V. L. Mathet, A. Sosnik, *J. Nanopart. Res.* **2013**, *15*, 1389.
[45] R. Glisoni, A. Sosnik, *J. Nanosci. Nanotechnol.* **2014**, *14*, 4670.
[46] M. L. Cuestas, V. Mathet, J. R. Oubiña, A. Sosnik, *Pharm. Res.* **2010**, *27*, 1184.
[47] X. Li, Y. Huang, X. Chen, Y. Zhou, Y. Zhang, P. Li, Y. Liu, Y. Sun, J. Zhao, F. Wang, *J. Drug Target.* **2009**, *17*, 739.
[48] A. Sosnik, G. Gotelli, G. A. Abraham, *Prog. Polym. Sci.* **2011**, *36*, 1050.
[49] M. A. Moretton, R. J. Glisoni, D. A. Chiappetta, A. Sosnik, *Colloids Surf. B: Biointerfaces* **2010**, *79*, 467.
[50] G. Gotelli, P. Bonelli, G. Abraham, A. Sosnik, *J. Appl. Polym. Sci.* **2011**, *121*, 1321.
[51] R. J. Glisoni, D. A. Chiappetta, A. G. Moglioni, A. Sosnik, *Pharm. Res.* **2012**, *79*, 739.
[52] P. Hole, K. Sillence, C. Hannell, C. M. Maguire, M. Roesslein, G. Suarez, S. Capracotta, Z. Magdolenova, L. Horev-Azaria, A. Dybowska, L. Cooke, A. Haase, S. Contal, S. Manø, A. Vennemann, J.-J. Sauvain, K. C. Staunton, S. Anguissola, A. Luch, M. Dusinska, R. Korenstein, A. C. Gutleb, M. Wiemann, A. Prina-Mello, M. Riediker, P. Wick, *J. Nanopart. Res.* **2013**, *15*, 2101.
[53] V. Filipe, A. Hawe, W. Jiskoot, *Pharm. Res.* **2010**, *27*, 796.
[54] X. Wang, O. Ramström, M. Yan, *J. Mater. Chem.* **2009**, *19*, 8944.
[55] J. H. Ahire, I. Chambrier, A. Mueller, Y. Bao, Y. Chao, *ACS Appl. Mater. Interface* **2013**, *5*, 7384.
[56] C. Lu, X. Chen, Z. Xie, T. Lu, X. Wang, J. Ma, X. Ji, *Biomacromolecules* **2006**, *7*, 1806.
[57] M. Tang, A. J. P. White, M. M. Stevens, C. K. Williams, *Chem. Commun.* **2009**, 941.
[58] A. Sosnik, D. Cohn, J. San Román, G. A. Abraham, *J. Biomater. Sci. Pol. Ed.* **2003**, *14*, 227.
[59] V. Bordegé, A. Muñoz-Bonilla, O. León, R. Cuervo-Rodríguez, M. Sánchez-Chaves, M. Fernandez-García, *J. Pol. Sci. Part A: Pol. Chem.* **2011**, *49*, 526.
[60] M. Bierenstiel, M. Schla, *Eur. J. Org. Chem.* **2004**, *7*, 1474.
[61] C. Zhang, Q. Ping, Y. Ding, *J. Appl. Pol. Sci.* **2005**, *97*, 2161.
[62] H. Fan, C. Wang, Y. Li, Y. Wei, *J. Memb. Sci.* **2012**, *415-416*, 161.
[63] Z. Takáts, K. Vékey, L. Hegeds, *Rap. Commun. Mass Spectrom.* **2001**, *15*, 805.
[64] K. Raith, C. E. H. Schmelzer, R. H. H. Neubert, *Int. J. Pharm.* **2006**, *319*, 1.
[65] D. Cohn, A. Sosnik, *J. Mater. Sci. Mater. Med.* **2003**, *14*, 175.
[66] D. Cohn, A. Sosnik, A. Levy, *Biomaterials* **2003**, *24*, 3707.
[67] D. Cohn, G. Lando, A. Sosnik, S. Garty, A. Levi, *Biomaterials* **2006**, *27*, 1718.
[68] I. J. Goldstein, C. E. Hollerman, E. E. Smith, *Biochemistry* **1965**, *4*, 876.
[69] W. I. Weis, K. Drickamer, *Annu. Rev. Biochem.* **1996**, *65*, 441.
[70] H. Meng-Xin, X. Zhi-Kang, *Colloids Surf. B: Biointerfaces* **2011**, *85*, 19.
[71] T. N. Kakuda, V. Sekar, L. Lavreys, E. De Paepe, T. Stevens, M. Vanstockem, T. Vangeneugden, R. M. Hoetelmans, *Clin. Pharmacol. Drug Dev.* **2014**, DOI: 10.1002/cpdd.88.
[72] Consolidated guidelines on the use of antiretroviral drugs for treating and preventing HIV infection: Summary of new recommendations. Geneva: OMS, **2013**. http://www. who. int/hiv/pub/guidelines/arv2013/art/arv2013_chapter07_low. pdf.
[73] A. Sosnik, D. A. Chiappetta, A. Carcaboso, *J. Control. Release* **2009**, *138*, 2.
[74] A. Sosnik, *Nanomedicine (Lond.)* **2010**, *5*, 833.
[75] A. Sosnik, A. Carcaboso, *Adv. Drug Deliv. Rev.* **2014**, *73*, 140.